POLITECNICO
MILANO 1863

Modeling Neurodegenerative Medical Diseases Using the Fisher-Kolmogorov Equation

Mario Capodanno

Valerio Grillo

Emanuele Lovino

Professor: Alfio Maria Quarteroni

Assistant Professor: Michele Bucelli

School of Industrial and Information Engineering

Master of Science – High Performance Computing Engineering

Index

Introduction

The increasing of neurodegenerative diseases is strictly linked to the continuous age trend of the world population. As people get older, these type of diseases will be more common, making it crucial to better understand them as they may remain asymptomatic for decades after the initial onset.

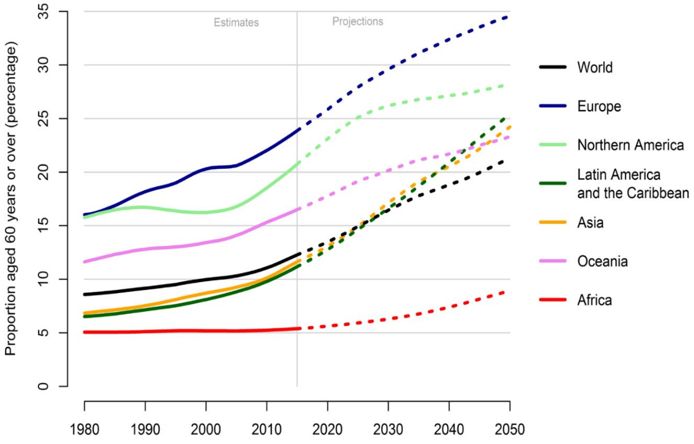

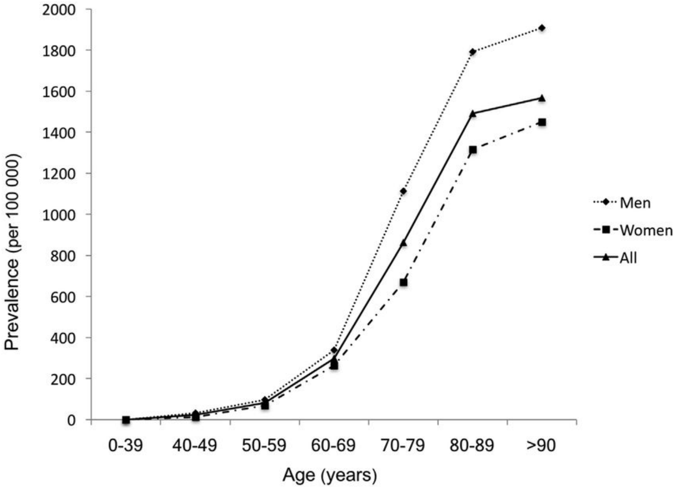

[1] Percentage of population aged 60 years or more according to region, from 1980 to 2050 Source: United Nations, World Population Prospects. The 2017 Revision
[2] Descriptive epidemiology of parkinsonism in the Canton of Geneva, Switzerland - Scientific Figure on ResearchGate.

Motivation & Aim

- Understand the dynamics of misfolded protein spreading (e.g., α-synuclein) in neurodegenerative diseases like Parkinson's and Alzheimer's.
- Implement a numerical solver to accurately simulate this protein aggregation and propagation.
- Verification of the solver on canonical test cases and after that, apply it to simulate protein dynamics within a 3D human brain mesh.

Mathematical Model

To model this complex phenomena of growth and spreading of misfolded proteins in the human brain, we consider the Fisher-Kolmogorov (FK) equation

$$\begin{cases} \dfrac{\partial c}{\partial t} = \mathrm{div}(\mathbf{D}\,\nabla c) + \alpha\, c\,(1-c) + f & \text{in } \Omega \times (0,T],\ \Omega \subset \mathbb{R}^d\ (d=2,3), \\ (\mathbf{D}\,\nabla c)\cdot \mathbf{n} = 0 & \text{on } \partial\Omega \times (0,T], \\ c(\mathbf{x},0) = c_0(\mathbf{x}) & \text{in } \Omega. \end{cases} \tag{1}$$

c(x, t):
Concentration of misfolded proteins (ranges from 0 to 1)

α:
Growth rate of the spreading process

f(x, t):
Forcing term

$\mathbf{D} = d_{\mathrm{ext}}\mathbf{I} + d_{\mathrm{axn}}(\mathbf{n}\otimes\mathbf{n})$

Diffusion tensor that describes how proteins spread in space.
d_{ext} is the isotropic diffusion.
d_{axn} is the anisotropic diffusion along axonal fiber directions.
n is the unit vector field showing the local axonal direction.

Homogeneous Neumann condition:
It prevents an outflow across the boundary.

[3] Weickenmeier, J., Jucker, M., Goriely, A., & Kuhl, E. *A physics-based model explains the prion-like features of neurodegeneration…* Journal of the Mechanics and Physics of Solids, 124 (2019), 264–281.

Assumptions

$\alpha \in L^\infty(\Omega)$.

$\mathbf{D} \in L^\infty(\Omega, \mathbb{R}^{d\times d})$ and $\exists d_0 > 0\ \forall \xi \in \mathbb{R}^d : d_0|\xi|^2 \leq \xi^T \mathbf{D} \xi\ \forall \xi \in \mathbb{R}^d$.

$f \in L^2((0,T]; L^2(\Omega))$.

$c_0 \in L^2(\Omega)$.

Under the given assumptions (with f **= 0** and ϕ_N **= 0**), the model admits **traveling wave solutions**.

$$c(x,t) = U(x - kt), \qquad k \in \mathbb{R}, \quad U\colon \mathbb{R} \to [0,1].$$

If the **initial condition** satisfies:
$0 \leq c_0(x) \leq 1$ for all x in the domain Ω,
then the **solution remains bounded**:
$0 \leq c(x,t) \leq 1$ for all $x \in \Omega$ and $t > 0$.

This setup leads to two **spatially uniform steady states**:

- **c = 0** → *unstable equilibrium*
- **c = 1** → *stable equilibrium*

[4] Corti, M., Bonizzoni, F., Dedè, L., Quarteroni, A.M., & Antonietti, P.F. Discontinuous Galerkin methods for the Fisher–Kolmogorov equation…Computer Methods in Applied Mechanics and Engineering, 417 (2023), 116450.
[5] Salsa, S. (2016). Introduzione. In Equazioni a derivate parziali, UNITEXT, vol 98. Springer, Milano.

Weak Formulation

By applying the assumptions on the domain and the homogeneous Neumann conditions, we derived the following weak formulation of the problem:

Let $v \in V = H^1(\Omega) = \{ v \in L^2(\Omega) \colon \nabla v \in L^2(\Omega) \}$.
$\forall t \in (0,T)$, find $c \in V$ such that:

$$\begin{cases} \displaystyle\int_\Omega \frac{\partial c}{\partial t} v \, d\Omega = \underbrace{- \int_\Omega \mathbf{D}\nabla c \cdot \nabla v \, d\Omega + \int_\Omega \alpha c(1-c) v \, d\Omega}_{\text{-b(c)(v)}} & \forall v \in V, \\ c(\mathbf{x},0) = c_0(\mathbf{x}) & \text{in } \Omega. \end{cases} \tag{3}$$

Now we write the above formulation in its residual form:

$\forall t \in (0,T)$, find $c \in V$ such that

$$\begin{cases} R(c)(v) = 0 & \forall v \in V, \\ c(\mathbf{x},0) = c_0(\mathbf{x}) & \text{in } \Omega. \end{cases} \tag{4}$$

$$\boxed{R(c)(v) = \int_\Omega \frac{\partial c}{\partial t} v \, d\Omega + b(c)(v)}$$

Semidiscrete Galerkin Formulation

- We now introduce a mesh $\mathcal{T}_h$ over the domain Ω and the finite element space:

$$X_h^r := \{v_h \in [\mathcal{C}^0(\Omega)]^d, \forall k \in \mathcal{T}_h, v_h|_k \in \mathbb{P}^r, r = 1\}.$$

and set $V_h = V \cap X_h^r, \dim(V_h) = N_h < +\infty,$

- The semi-discrete formulation reads:

$\forall t \in (0,T),$ find $c_h(t) \in V_h$ such that:

$$\begin{cases} R(c_h)(v_h) = 0 & \forall v_h \in V_h, \\ c_h(\mathbf{x}, 0) = c_{0,h}(\mathbf{x}) & \text{in } \Omega. \end{cases} \quad (5)$$

Fully Discrete Galerkin Formulation

We now discretize through time by using the **Implicit Euler method**. Let us partition the interval $[0, T]$ into the subintervals $(t_n, t_{n+1}]$ with $n = 0, 1, \ldots, N_{T-1}, t_{N_T} = T$.
Each sub-interval has length Δt. We denote with a superscript n the approximate solution at time t_n, i.e. $c_h^n \approx c_h(t_n)$.

$$\underbrace{\int_\Omega \frac{c_h^{n+1} - c_h^n}{\Delta t} v_h \, d\Omega + b(c_h^{n+1})(v_h)}_{R^{n+1}(c_h^{n+1})(v_h)} = 0 \quad \forall v_h \in V_h, \quad n = 0, 1, \ldots, N_{T-1}. \qquad (6)$$

Numerical Modeling (3)

Being (6) a non-linear problem, we employ Newton's method for its solution. We firstly introduce the **Fréchet** derivative:

For a given functional $G : V \to \mathbb{R}$ the derivative at a point $u \in V$ is a linear operator $A(u) = \dfrac{dG}{du} : V \to \mathbb{R}$ such that

$$\lim_{\|\delta\| \to 0} \frac{|G(u+\delta) - G(u) - A(u)(\delta)|}{\|\delta\|} = 0.$$

In our case we compute the derivative $a(c_h^{n+1})(\delta_h, v_h)$ of the discrete residual $R^{n+1}(c_h^{n+1})(v_h)$

$$a(c_h^{n+1})(\delta_h, v_h) = \int_\Omega \frac{\delta_h}{\Delta t} v_h \, d\Omega + \int_\Omega \mathbf{D}\nabla\delta_h \cdot \nabla v_h \, d\Omega - \int_\Omega \alpha\delta_h(1 - 2c_h^{n+1}) v_h \, d\Omega.$$

[5] Salsa, S. (2016). Introduzione. In Equazioni a derivate parziali, UNITEXT, vol 98. Springer, Milano.

Numerical Modeling (4)

Algorithm 1 Newton's Method at Time Step $n+1$

Require: Previous solution c_h^n, tolerance `tol`, maximum iterations `max_iter`
Ensure: Updated solution c_h^{n+1}

  Initialize $c_h^{n+1,(0)} \leftarrow c_h^n$
  for each $k = 0, 1, 2, \ldots,$ `max_iter` **do**
    Assemble and solve the linear system:

$$a(c_h^{n+1,(k)})(\delta_h^{(k)}, v_h) = -R(c_h^{n+1,(k)})(v_h) \quad \forall v_h \in V_h$$

    Update: $c_h^{n+1,(k+1)} \leftarrow c_h^{n+1,(k)} + \delta_h^{(k)}$
    if $\|\delta_h^{(k)}\| <$ `tol` **then**
      break
    end if
  end for
  return $c_h^{n+1} \leftarrow c_h^{n+1,(k+1)}$

Error and stability expected properties (1)

Stability of semi-discrete formulation

In this context, **boundedness does not** necessarily **imply stability** due to the non-linear nature of the problem. Although we do not provide a formal proof of stability here, we **assume** it as a necessary condition for convergence.

Stability of fully-discrete formulation

Since Backward-Euler method was used for the discretization with respect to time of the problem, we have **unconditionally stability** $\forall \Delta t \geq 0$.

[6] Quarteroni, A., Numerical Models for Differential Problems, Editore: Springer, Anno edizione: 2017

Error and stability expected properties (2)

Convergence

- ***General estimate***

$$\left\| c(t^{(k)}) - c_h(t^{(k)}) \right\|^2_{L^2(\Omega)} \le C\left(h^{\,r} + \Delta t^{\,p(\vartheta)}\right).$$

Where C is a constant, independent of the discretization parameters h and Δt; it typically depends only on the problem data (e.g., coefficients, domain geometry, final time T) and on the regularity of the exact solution c.

Here $k = 0, 1, \dots, N$ is the discrete time-step index defined by: $t^{(k)} = t_0 + k \cdot \Delta t$,

where $\Delta t = T / N$ denotes the uniform time-step size on the interval $(0, T)$, and $t_0 = 0$.

- ***Estimate for linear elements and backward Euler***

For linear finite elements $(r = 1)$ and the backward-Euler time discretization $(p(\vartheta) = 1)$

$$\left\| c(t^{(k)}) - c_h(t^{(k)}) \right\|^2_{L^2(\Omega)} \le C\left(h + \Delta t\right).$$

[6] Quarteroni, A., Numerical Models for Differential Problems, Editore: Springer, Anno edizione: 2017

Software Implementation (1)

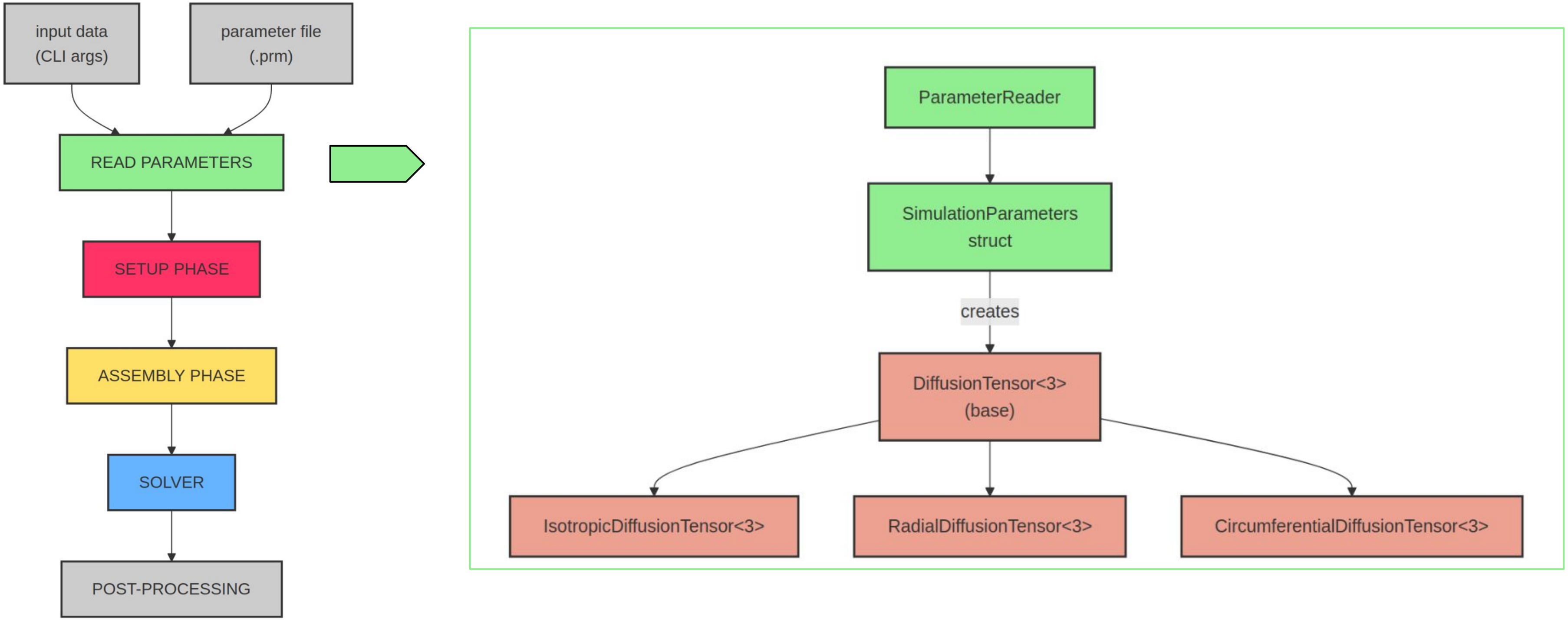

Software Implementation (2)

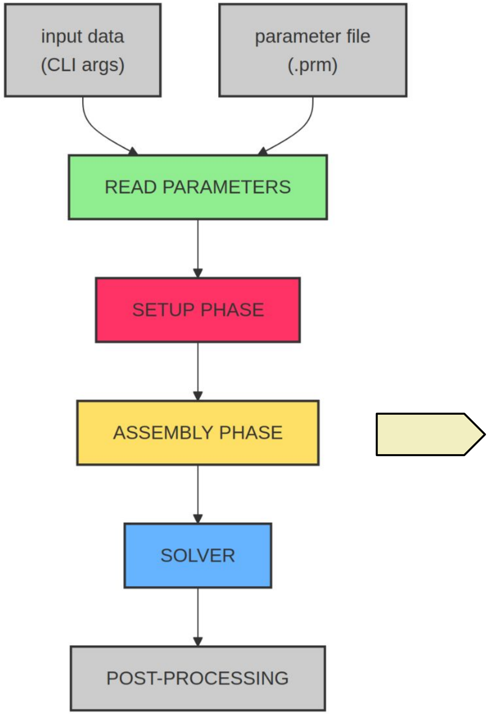

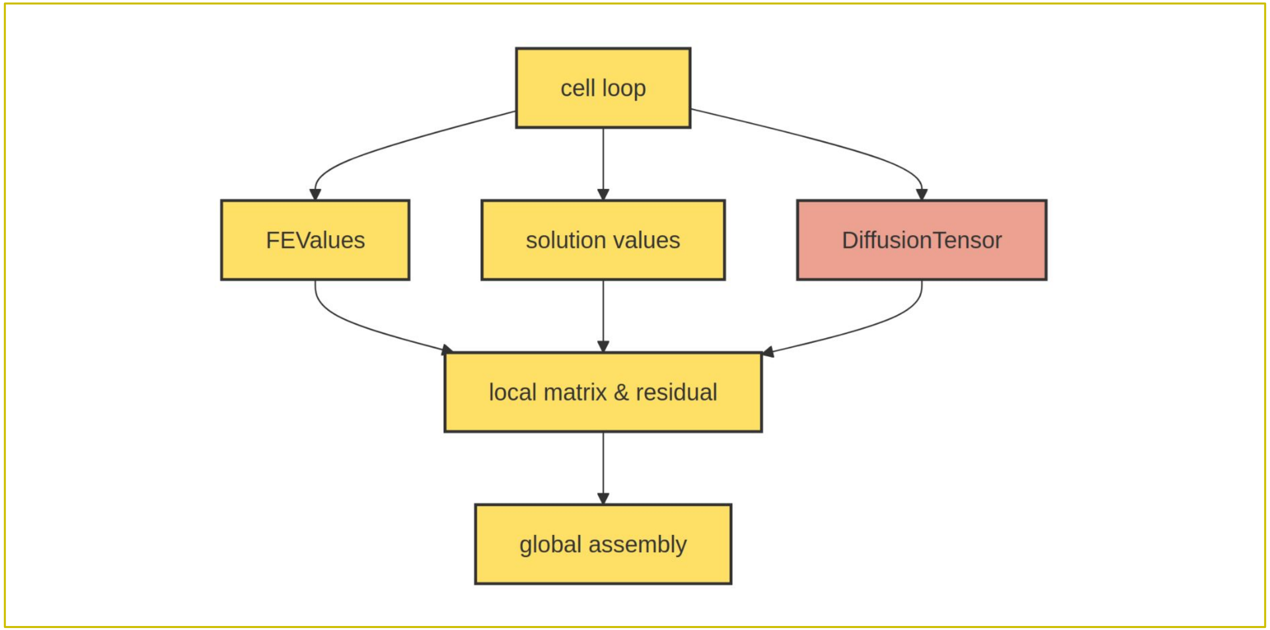

Prion-like spreading in 1D

To visualize the spatio-temporal dynamics that emerge from the Fisher–Kolmogorov reaction–diffusion model,

$$\frac{\partial c}{\partial t} = d\,\frac{\partial^2 c}{\partial x^2} + \alpha\, c\,(1-c), \qquad (9)$$

we solved (9) in the one–dimensional domain $\Omega = \{x \mid -1 \leq x \leq 1\}$ over the time interval $\mathcal{T} = \{t \mid 0 \leq t \leq 20\}$.

Spatial and temporal discretizations. The domain was partitioned into $N = 200$ linear elements, while the interval $\mathcal{T}$ was divided into $n_{\text{step}} = 200$ uniform steps of size $\Delta t = 0.1$.

Parametric variation. We explored the sensitivity of the solution to

- *growth*: $\{1\alpha,\, 2\alpha,\, 4\alpha\}$ with $\alpha = 1$;
- *spreading* (diffusivity): $\{1d,\, 2d,\, 4d\}$ with $d = 10^{-4}$.

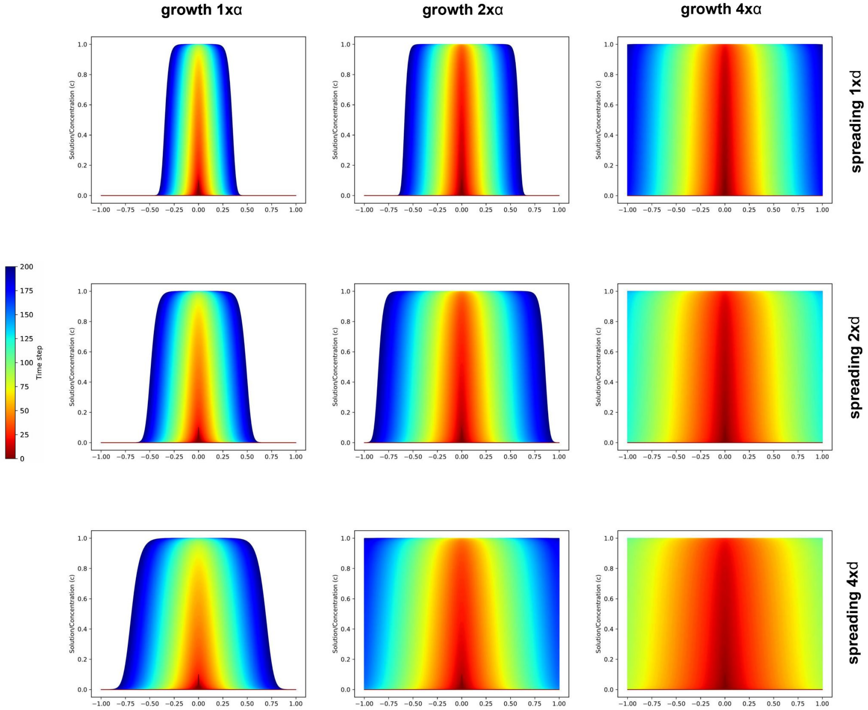

[3] Weickenmeier, J., Jucker, M., Goriely, A., & Kuhl, E. *A physics-based model explains the prion-like features of neurodegeneration*… Journal of the Mechanics and Physics of Solids, 124 (2019), 264–281.

Convergence Analysis in 3D

To assess the spatial accuracy of our formulation in three space-dimensions we use a unitary cubic domain $\Omega = (0,1)^3$.

Spatial and temporal discretizations. The cube is partitioned with a sequence of *tetrahedral* elements generated with GMSH. The representative element sizes are $h = \{0.5, 0.25, 0.125, 0.0625, 0.03125\}$, so that each successive mesh is obtained by uniform refinement. Unless otherwise stated, we use continuous, piecewise-polynomial finite-element spaces of degree $r = 1$. Time is advanced by a backward Euler step of size $\Delta t = 0.01$, resulting in $n_{\text{step}} = 100$ uniform steps ($T = 1.0$).

Manufactured solution and parameters. Following Corti *et al.* [2], we prescribe the exact solution

$$c_{\text{ex}}(x,y,z,t) = \big(\cos(\pi x)\cos(\pi y)\cos(\pi z)\big)\,\mathrm{e}^{-t}, \tag{10}$$

and choose an *isotropic* diffusion tensor $\mathbf{D} = d_{\text{ext}}\mathbf{I}$ with $d_{\text{ext}} = 1$ and reaction coefficient $\alpha = 0.1$. The forcing term is obtained by substitution of (10) into the equation (10).

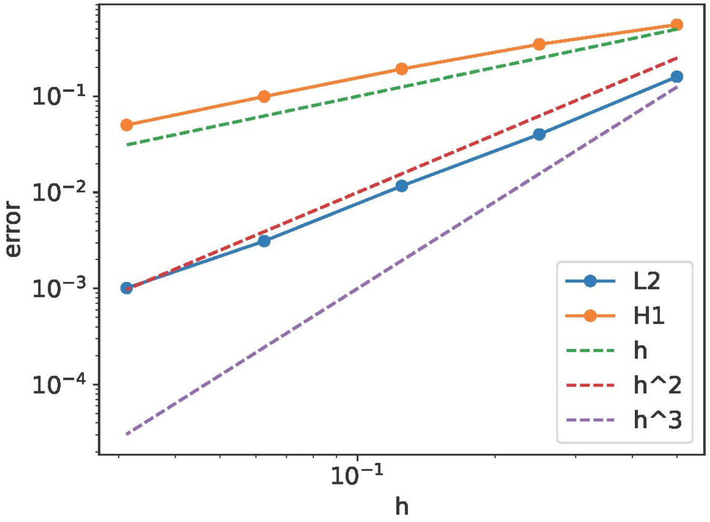

The above figure plots the e_{L^2} and e_{H^1} errors versus h on log–log axes together with the reference slopes h, h^2 and h^3. For the linear space ($r = 1$) we observe:

[4] Corti, M., Bonizzoni, F., Dedè, L., Quarteroni, A.M., & Antonietti, P.F. Discontinuous Galerkin methods for the Fisher–Kolmogorov equation…Computer Methods in Applied Mechanics and Engineering, 417 (2023), 116450.

1 - Half-Brain Mesh in 3D

Spatio-temporal evolution of the scalar field c(x, t) on a human brain-hemisphere mesh.

Geometry	Right-hemisphere tetrahedral mesh (**brain-h3.0.msh**).
Diffusion mode	**Isotropic** – expected to spread tangentially and uniformly.
Initial seed	High concentration c = 0.9 inside a cube (approx Dorsal Motor Nucleus); c = 0 elsewhere.
Boundary condition	Homogeneous Neumann on the outer cortical surface.

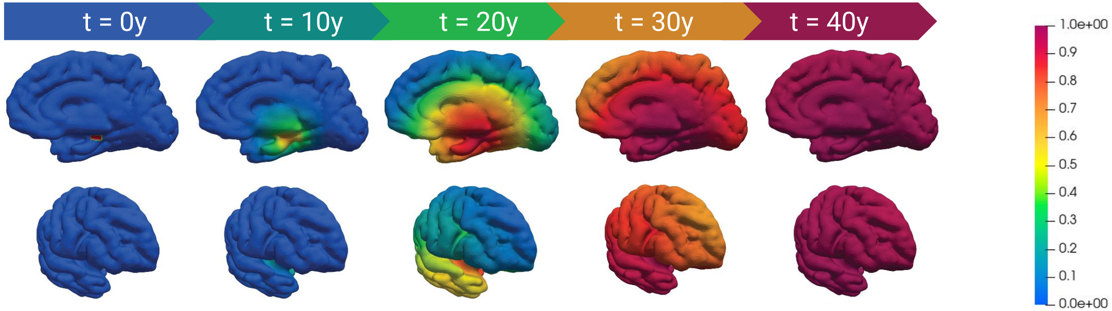

2 - Half-Brain Mesh in 3D

To verify how the geometry of the diffusion tensor ***D(x)*** shapes the propagation, we repeated the simulation with three prototypical tensors while keeping every kinetic parameter fixed. In addition to the baseline case ***isotropic***, we also considered the tensors ***circumferential*** and ***radial***.

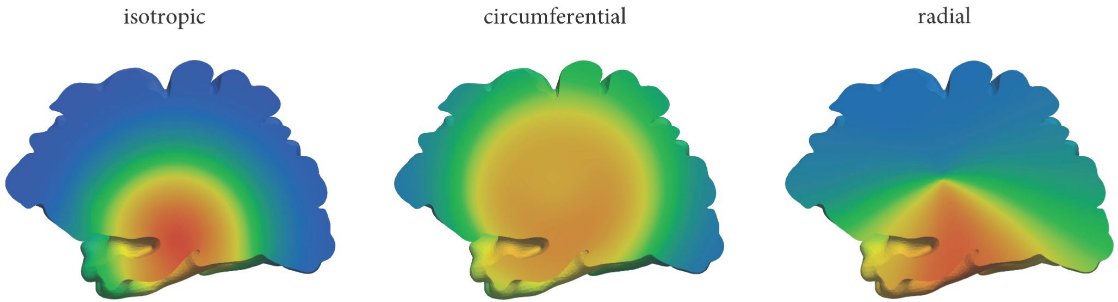

The above resulting concentration fields at the intermediate time **t = 16y**, show the differences each transport tensor produces before global saturation occurs but well after the initial transients have decayed.

[3] Weickenmeier, J., Jucker, M., Goriely, A., & Kuhl, E. *A physics-based model explains the prion-like features of neurodegeneration…* Journal of the Mechanics and Physics of Solids, 124 (2019), 264–281.

Execution Time Analysis

Single-node simulations

Workstation equipped with an 11th Gen Intel Core i7-1165G7 processor (2.80 GHz) and 16 GB of RAM. Each run was invoked using the mpirun *--use-hwthread-cpus* option to exploit all available threads.

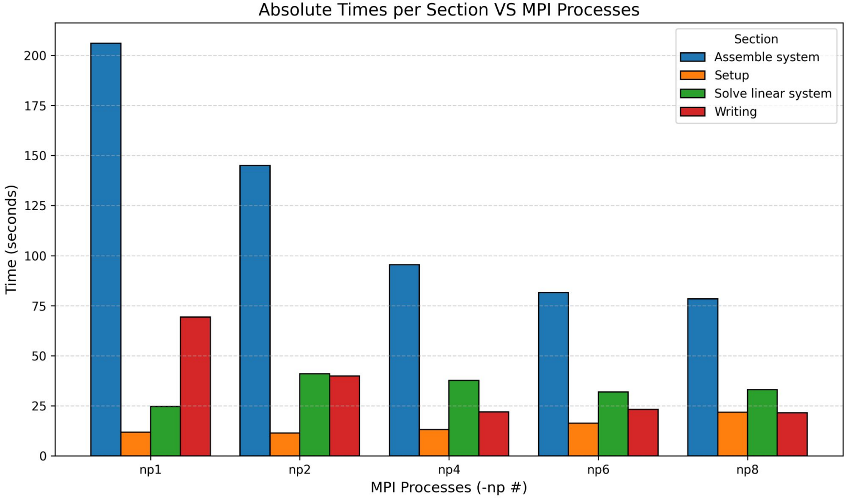

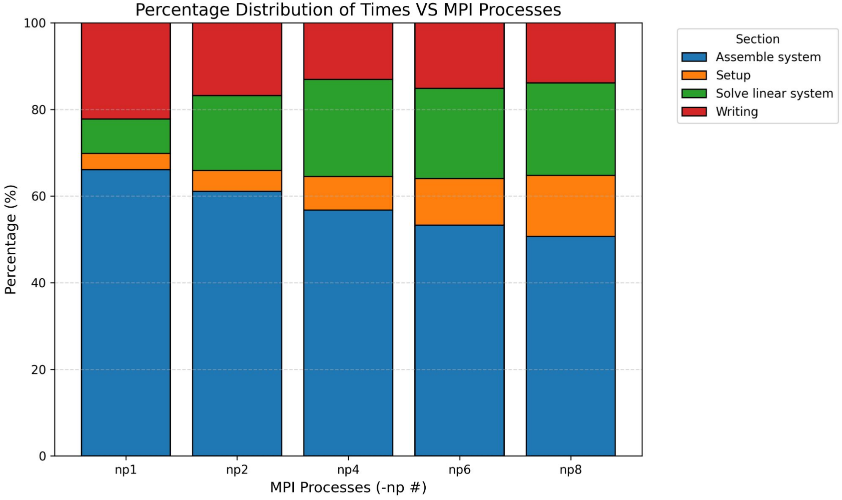

Summary of Our Work

- Developed a **numerical solver** for the **Fisher–Kolmogorov equation**, modeling the spread of **α-synuclein proteins** in neurodegenerative diseases like **Alzheimer's** and **Parkinson's**.
- Derived both **semi-discrete** and **fully discrete** formulations, and solved the **nonlinear problem** using **Newton's method**.
- Verification of the model in **1D**, following the primary reference, then extended to **3D** using a cubic domain.
- **Convergence tests** confirmed expected **theoretical accuracy**.
- Simulated protein spreading in a **realistic 3D brain hemisphere mesh**, enhancing the biological relevance of the model.

References

[1] Percentage of population aged 60 years or more according to region, from 1980 to 2050 Source: United Nations, World. Population Prospects. The 2017 Revision

[2] Descriptive epidemiology of parkinsonism in the Canton of Geneva, Switzerland - Scientific Figure on ResearchGate.

[3] Weickenmeier, J., Jucker, M., Goriely, A., & Kuhl, E.
A physics-based model explains the prion-like features of neurodegeneration…
Journal of the Mechanics and Physics of Solids, 124 (2019), 264–281.
https://doi.org/10.1016/j.jmps.2018.10.013

[4] Corti, M., Bonizzoni, F., Dedè, L., Quarteroni, A.M., & Antonietti, P.F.
Discontinuous Galerkin methods for the Fisher–Kolmogorov equation…
Computer Methods in Applied Mechanics and Engineering, 417 (2023), 116450.
https://doi.org/10.1016/j.cma.2023.116450

References

[5] Salsa, S. (2016).
Introduzione. In *Equazioni a derivate parziali*, UNITEXT, vol 98. Springer, Milano.
https://doi.org/10.1007/978-88-470-5785-2_1

[6] Quarteroni, A., Numerical Models for Differential Problems, Editore: Springer, Anno edizione: 2017

[7] deal.II Developers.
The deal.II Library: Reference Documentation, version 9.6.0, 2024.
https://www.dealii.org